BMC Cancer

RESEARCH Open Access

Serum metabolomics analysis of malnutrition in patients with gastric cancer: a cross sectional study

Liang Fu[1,2], Lixin Song[3], Xi Zhou[4], Lin Chen[2], Lushan Zheng[1], Dandan Hu[1], Sha Zhu[1], Yanting Hu[5], Daojun Gong[6], Chun-Liang Chen[3], Xianghong Ye[1*] and Shian Yu[7*]

Abstract

Background Although malnutrition is common in cancer patients, its molecular mechanisms has not been fully clarified. This study aims to identify significantly differential metabolites, match the corresponding metabolic pathways, and develop a predictive model of malnutrition in patients with gastric cancer.

Methods In this cross-sectional study, we applied non-targeted metabolomics using liquid chromatography-mass spectrometry to explore the serum fingerprinting of malnutrition in patients with gastric cancer. Malnutrition-specific differential metabolites were identified by orthogonal partial least-squares discriminant analysis and t-test and matched with the Human Metabolome Database and the LIPID Metabolites and Pathways Strategy. We matched the corresponding metabolic pathways of malnutrition using pathway analysis at the MetaboAnalyst 5.0. We used random forest analyses to establish the predictive model.

Results We recruited 220 malnourished and 198 non-malnourished patients with gastric cancer. The intensities of 25 annotated significantly differential metabolites were lower in patients with malnutrition than those without, while two others were higher in patients with malnutrition than those without, including newly identified significantly differential metabolites such as indoleacrylic acid and lysophosphatidylcholine(18:3/0:0). We matched eight metabolic pathways associated with malnutrition, including aminoacyl-tRNA biosynthesis, tryptophan metabolism, and glycerophospholipid metabolism. We established a predictive model with an area under the curve of 0.702 (95% CI: 0.651–0.768) based on four annotated significantly differential metabolites, namely indoleacrylic acid, lysophosphatidylcholine(18:3/0:0), L-tryptophan, and lysophosphatidylcholine(20:3/0:0).

Conclusions We identified 27 specific differential metabolites of malnutrition in malnourished compared to non-malnourished patients with gastric cancer. We also matched eight corresponding metabolic pathways and developed a predictive model. These findings provide supportive data to better understand molecular mechanisms of malnutrition in patients with gastric cancer and new strategies for the prediction, diagnosis, prevention, and treatment for those malnourished.

*Correspondence:
Xianghong Ye
13868992616@163.com
Shian Yu
ysa513@163.com

Full list of author information is available at the end of the article

Keywords Gastric cancer, Malnutrition, Metabolomics, Metabolite, Metabolic pathways, Predictive model

Background

Gastric cancer is the 5th most common type of cancer globally and 2nd in China [1–3]. Gastric cancer-caused cancer deaths rank fourth globally and third in China [1–3]. The improvement in diagnosis and treatment has prolonged the survival of patients with gastric cancer. A systematic review of international studies found a 5-year survival rate of 72.1% in patients with gastric cancer [4]. Another systematic review showed that in China, the pooled one-, two-, three- and five-year survival rates of gastric cancer were 75.4%, 54.3%, 53.4%, and 44.5%, respectively [5]. However, patients often face various critical challenges during cancer survivorship, including malnutrition, in which more than 60.0% of patients living with gastric cancer receive a diagnosis [6, 7]. Malnutrition is significantly associated with poor quality of life [8, 9], early cessation of anti-neoplastic treatment [8], high incidence of incisional infection [10], extended hospital stay [11], shortened overall and disease-free survival [8, 10, 11], and increased medical costs [10–12].

Malnutrition, also known as undernutrition, results from a lack of intake or nutrition uptake, leading to altered body composition (decreased fat-free mass) and body cell mass, diminished physical and mental functions, and clinical outcomes [13]. According to the Global Leadership Initiative on Malnutrition (GLIM), a malnutrition diagnosis should meet at least one of the three phenotypic criteria (weight loss of more than 5% within the past six months, or more than 10% beyond six months; body mass index (BMI) less than 18.5 kg/m^2 if under 70 years old, or less than 20 kg/m^2 if 70 years or older (Asia); and reduced muscle mass) and one of the two etiologic criteria (reduced food intake or assimilation, and inflammation) [14]. Although malnutrition is common in cancer patients [15], its molecular mechanisms has not been fully clarified. The currently identified reasons for developing malnutrition include immune response, systemic inflammation, symptoms, worsened systemic inflammation due to spillover of tumor-derived cytokines, hypoxic stress in the tumor microenvironment, and indirect effects of cancer or its treatments [16].

The metabolomics approach can identify and determine the metabolites in biological samples under normal conditions compared to altered states [17]. As a phenotypic analysis tool and rapidly emerging as a primary research method in tumor biomarkers [17, 18], several studies have applied metabolomics to identify cachexia biomarkers in patients with cancer - a synonym of chronic disease-related malnutrition [19–21]. Cancer cachexia, a specific form of chronic disease-related malnutrition with inflammation, which is diagnosed by a weight loss of more than 5% over the past 6 months, or a BMI of less than 20 kg/m^2 with any degree of weight loss over 2%, or an appendicular skeletal muscle index consistent with sarcopenia and any degree of weight loss over 2% [20, 22]. Research to date has explored differential metabolites, corresponding metabolic pathways, and predictive models of cachexia in patients with cancer. Studies have indicated that some metabolites, arginine, citrulline, histidine [23, 24], lysophosphatidylcholine (LysoPC)(15:0) [25, 26], alanine, and choline [27, 28], were significantly associated with cachexia in patients with cancer, and alanine, aspartate, glutamate metabolism, and arginine, and proline metabolism were commonly involved in the metabolic pathways [23, 24, 28, 29]. A model for cachexia diagnosis in patients with cancer was created based on carnosine, leucine, and phenyl acetate with an area under the curve of 0.991 in a previous study [28]. These findings provided a good reference for the mechanism understanding and management of cachexia in patients with cancer.

Although cachexia falls under the umbrella of malnutrition, the methods used to diagnose cachexia and malnutrition are distinct [14, 22, 30], and thus, the metabolomics results of cachexia in cancer patients cannot fully reflect the differential metabolites, corresponding metabolic pathways, and predictive models of malnutrition in patients with cancer. In addition, little research has examined metabolomics in patients with gastric cancer. Therefore, this study aimed to identify significantly differential metabolites, match the corresponding metabolic pathways, and develop a predictive model of malnutrition in patients with gastric cancer by non-targeted metabolomics using liquid chromatography-mass spectrometry (LC-MS).

Materials and methods

Study design and participants

This cross-sectional study occurred in a comprehensive hospital in southeast China. Patients with gastric cancer were eligible if they: (1) were aged 18 years or above; (2) had been diagnosed with gastric cancer; (3) reported an Eastern Cooperative Oncology Group Performance Status (ECOG-PS) score < 4; (4) planned to undergo antitumor surgery or completed antitumor surgery; and (5) had not received any treatment for gastric cancer at this admission. All eligible participants should be able to provide informed consent. We excluded patients with gastric cancer if they (1) had uncontrolled diabetes mellitus, (2) received glucocorticoid therapy, (3) had liver and/or renal failure, and (4) had other conditions not suitable for inclusion in the study. From December 2020 to May

2022, we recruited patients with gastric cancer from the Department of Gastrointestinal Surgery, Department of Hepatobiliary and Pancreatic Surgery, and Department of Medical Oncology, Jinhua Municipal Central Hospital.

Measurements

We reviewed the electronic medical record to collect general information, including gender, age (years), cancer stage, duration since diagnosis (days), nutritional therapy within the past month, and cancer therapy phase. Patients or caregivers reported the patient's weight (kilogram), educational level, occupation status, marital status, residence status, and financial stress. Research nurses measured patients' body mass index, left calf circumference, and ECOG-PS score.

We diagnosed malnutrition using GLIM criteria with Nutritional Risk Screening 2002 (NRS 2002) and at least one phenotypic criterion and one etiologic criterion should be present [14, 31]. Three phenotypic criteria were (1) weight loss >5% within the past six months, or >10% beyond six months (2) BMI <18.5 kg/m^2 if <70 years, or <20 kg/m^2 if ≥70 years (Asia), and (3) reduced muscle mass (i.e., the left calf circumference (CC) <30 cm for males or <29.5 cm for females). Two etiologic criteria were (1) reduced food intake or assimilation and (2) inflammation. We identified gastric cancer as reduced food intake or assimilation.

Sample collection

Study participants fasted and provided 2 mL of venous blood, which we collected with a non-anticoagulant vacuum collection vessel (Beikete, Wenzhou, Zhejiang, China) under aseptic conditions. Blood samples were allowed to stand at room temperature for 30 min and then centrifuged at 2390 (×g) at 4℃ for 10 min to obtain serum samples. We stored the serum samples in the −80℃ refrigerator until LC-MS analysis.

Materials for LC-MS analysis

We purchased LC-MS grade methanol and acetonitrile from Merck Company Inc. (Darmstadt, Germany). The chemical formic acid was MS grade and purchased from Fisher Scientific Company Inc. (Fairlawn, New Jersey, United States). All other reagents were of analytical grade. Ultra-pure water (18.2 MΩ) was prepared daily with a Milli-Q water purification system (Millipore, Milford, Massachusetts, United States).

Serum preparation for metabolome analysis

We vortexed 200 μL serum for 3 min with 600 μL of acetonitrile to remove the protein. The mixture underwent centrifugation for 10 min (15620 (×g), 4 °C). We dried 400 μL supernatant under nitrogen gas. Before the LC-MS analysis, residues were reconstituted and re-dissolved in 100 μL acetonitrile/water (1:1, v/v) solvent.

Instruments and condition

We performed chromatographic separation on an ExionLC system (AB Sciex, Foster City, California, USA). We applied a Waters Acquity BEH C18 column (2.1×100 mm, 1.7 μm) at the temperature of 35℃. The mobile phase A was water with 0.1% formic acid (v/v), and B was acetonitrile. We optimized the gradient as follows: 0–8 min from 5 to 60% B, 8–18 min from 60 to 97% B, 18–21 min at 97% B, then back to the initial ratio of 5% B and maintained with additional 4 min for re-equilibration. The injection volume of all samples was 2 μL.

We used an X500B Q-TOF mass spectrometer (AB Sciex, Foster City, California, USA) with an electrospray ionization source (Turbo Ionspray) for high-resolution detection. We implemented MS detection in both negative and positive ion modes. The mass spectrometer parameters were summarized: gas1 and gas2, 55 psi; curtain gas, 35 psi; heat block temperature, 550 ℃; ion spray voltage, -4.5 kV in negative mode and 5.5 kV in positive; delustering potential, 60 V; collision energy, ±35 V; and the collision energy spread was ±15 V. To monitor the reproducibility and stability of the acquisition system, quality control (QC) samples were prepared by pooling small aliquots of each sample. The QC specimens were analyzed every five samples throughout the whole analysis procedure.

Statistical analysis

We uploaded the raw data to the MarkerView 1.3.1 software for data extraction. After data pretreatment, we obtained a three-dimensional matrix of sample names (observations), annotated peak indices (RT-m/z pairs), and peak intensities. We calibrated the peak intensity by the internal standard. We excluded variates with relative standard deviation (RSD) ≥ 40% in QCs. We exported the final matrix to a Microsoft Excel file, performed normalization by sum, and uploaded the pretreated data into SIMCA 14.1 for multivariate data analysis. We first established the principal component analysis (PCA) models containing all samples to observe the gathering of QCs and the distance among the three groups. QCs closely gathered means the satisfactory reproducibility and stability of the acquisition system. Orthogonal partial least-squares discriminant analysis (OPLS-DA) is a statistical method of supervised discriminant analysis. We included the grouping variables in the modeling for pairwise analysis to screen different metabolites and to examine group differences. To prevent overfitting, we used 7-fold cross-validation and 200 response permutation testing to evaluate the quality of the model. The permutation test results implied the OPLS-DA models' satisfied validity if

the blue regression line of the Q^2 points was below zero. We calculated the variable importance in the projection (VIP) value of each variable in the OPLS-DA model to indicate its contribution to the classification. Metabolites with the VIP value > 1 as well as |p(correlation)| >0.2 were further applied to a t-test to measure the significance of each metabolite; $p < 0.05$ was considered statistically significant. We imported the accurate masses of the differential metabolites into the Human Metabolome Database and the LIPID Metabolites and Pathways Strategy, setting the molecular weight tolerance to ±10 ppm. Several eligible metabolites were identified through these databases. First, we confirmed whether each metabolite was endogenous. Then, we compared the actual MS/MS spectra with the predicted LC-MS/MS spectra in the databases. To annotate a molecule as the corresponding metabolite, at least two or more ion fragments needed to match. We drew volcano plot, heatmaps, and box-and-whisker plots in R software (4.1.2) with the ggplot2, ggrepel, and pheatmap package. We matched the related metabolic pathways of malnutrition in patients with gastric cancer at the MetaboAnalyst 5.0 (http://www.MetaboAnalyst.ca/). The differential metabolite names companied with corresponding intensities of each sample were exported to the website.

To establish a predictive model, we used the randomForest package in R (4.1.2) to establish the random forest classification model. We randomly divided the data containing group information, sample names, and significantly differential metabolite intensities into two pieces, with 70% in the training set and 30% in the test set. We optimized the random forest classification prediction model by various parameters, including mtry, maxnodes, nodesize and ntree, and then output the important parameters of each variable. The receiver operating characteristic (ROC) curve (pROC package) represented the predictive ability of the random forest model.

Results

Participant demographic and clinical characteristics

We recruited a total of 418 patients with gastric cancer. 220 (52.6%) of the 418 patients with gastric cancer had malnutrition. 143 (65.0%) of those who were malnourished and 151 (76.3%) of those who were not malnourished were male. Their respective median ages (in years) were 69.0 and 65.0. Of the malnourished and non-malnourished patients with gastric cancer, 114 (51.8%) and 80 (40.4%) were stage III tumors, respectively, and the median duration since diagnosis was 40.5 and 82.0 days, respectively. Table 1 here.

Data pretreatment reproducibility and stability of the LC-MS analysis method

Figure S1 shows the base peak chromatograms (BPC) of quality controls in positive and negative ion modes. The chromatographic peaks were evenly distributed and clearly separated. The PCA plots of all samples in negative and positive ion modes showed the QC samples gathered near the center, indicating good stability and reproducibility of this experiment. The R^2X (cum) values of the positive ion mode were 0.879 and 0.835, respectively. Figure S2(A). According to the dot plots, QC distribution was also the most clustered. See Figure S2(B). The above results indicate that the instruments and methods were relatively stable during the experiment.

Significantly differential metabolites between malnourished and non-malnourished patients with gastric cancer

Figure 1(A) show the OPLS-DA score plots of comparisons between gastric cancer patients with and without malnutrition. The compared groups could be distinguished. The R^2Y (cum) and Q^2 (cum) of the positive ion mode were 0.698 and 0.430, respectively, while in the negative ion mode, they were 0.441 and 0.328, indicating apparent separation. Meanwhile, the permutation test results implied satisfactory validity of the OPLS-DA models as the blue regression line of the Q^2 points was below zero. See Fig. 1(B). We identified 172 significantly differential metabolites (VIP > 1, |p(correlation)| >0.2, and $p < 0.05$) between malnourished and non-malnourished patients with gastric cancer, 27 of which were annotated in the Human Metabolome Database and the LIPID Metabolites and Pathways Strategy (Fig. 2). Compared to those without malnutrition, malnourished patients with gastric cancer had lower intensities of 25 annotated significantly differential metabolites, indoleacrylic acid, 2-methylbutyroylcarnitine, phenylalanylphenylalanine, L-tryptophan, 1-O-hexadecyl-sn-glycero-3-phosphocholine, indole-3-carboxaldehyde, L-tyrosine, leucylalanine, glutamylleucine, N-sulfotyrosine, gamma-CEHC, testosterone sulfate, androsterone sulfate, pregnenolone sulfate, pregnanolone sulfate, N-palmitoyl arginine, LysoPE(18:3/0:0), LysoPE(18:2/0:0), LysoPE(18:1/0:0), LysoPE(20:3/0:0), LysoPC(16:1/0:0), LysoPC(18:3/0:0), LysoPC(18:0/0:0), LysoPC(20:5/0:0), and LysoPC(20:3/0:0), and higher intensities of two annotated significantly differential metabolites, hydroxybutyric acid and palmitoleic acid. See Figs. 3 and 4; Table 2.

Metabolic pathways associated with malnutrition in patients with gastric cancer

We matched eight metabolic pathways associated with malnutrition in patients with gastric cancer, including aminoacyl-tRNA biosynthesis; tryptophan metabolism;

Table 1 Demographic and clinical characteristics of the sample

Characteristics	Malnutrition (*N* = 220)		Non-malnutrition (*N* = 198)	
	n	%	*n*	%
Gender				
Male	143	65.0	151	76.3
Female	77	35.0	47	23.7
Age, year, median (25th-75th percentile)	69.0	59.0–73.0	65.0	55.0–70.0
<70	115	52.3	140	70.7
≥70	105	47.7	58	29.3
Weight, kilogram, median (25th-75th percentile)	50.0	45.6–56.8	60.0	55.0-67.3
Body mass index				
<18.5	108	49.1	0	0.0
≥18.5	112	50.9	198	100.0
Left calf circumference, centimeter, median (25th-75th percentile)[a]	31.0	29.7–32.9	34.3	32.6–36.2
Education level[a]				
Primary school or below	131	59.5	105	53.0
High school	70	31.8	80	40.4
University or above	9	4.1	10	5.1
Occupation status[a]				
Unemployed	145	65.9	124	62.6
Employed	65	29.5	71	35.9
Marital status[a]				
Single	19	8.6	13	6.6
Married	191	86.8	182	91.9
Solitude[a]				
No	195	88.6	182	91.9
Yes	15	6.8	13	6.6
Financial pressure[a]				
Not at all	108	49.1	100	50.5
A little bit	60	27.3	63	31.8
Somewhat	27	12.3	19	9.6
Very much	15	6.8	13	6.6
ECOG-PS score[a]				
0	35	15.9	109	55.1
1	116	52.7	71	35.9
2	37	16.8	11	5.6
3	22	10.0	4	2.0
Cancer stage[b]				
I	32	14.5	40	20.2
II	51	23.2	50	25.3
III	114	51.8	80	40.4
IV	18	8.2	22	11.1
Duration since diagnosis, day, median (25th-75th percentile)[d]	40.5	26.8-189.3	82.0	-1.0-479.8
Nutritional therapy (Past one month)[c]				
None	101	45.9	146	73.7
Yes	83	37.7	35	17.7
Cancer therapy phase				
Before operation	43	19.5	77	38.9
After operation before chemotherapy	104	47.3	26	13.1
After operation undergoing chemotherapy	33	15.0	37	18.7
After operation after chemotherapy	40	18.2	58	29.3

[a] $n = 405$, [b] $n = 407$, [c] $n = 365$, [d] $n = 386$

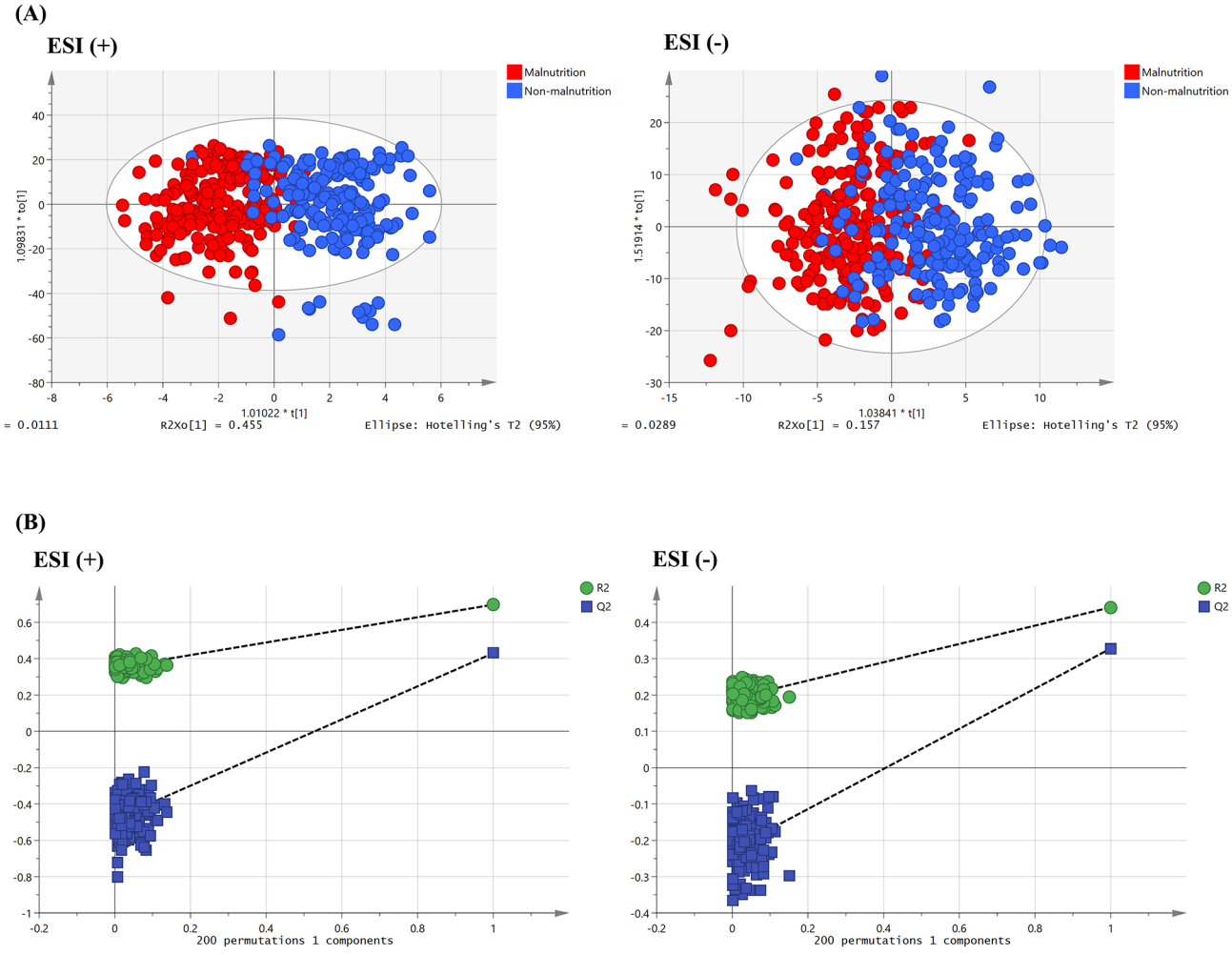

Fig. 1 Exploratory multivariate statistical analysis. (**A**) Orthogonal partial least-squares discriminant analysis (OPLS-DA) score plots between malnourished (red dots) and non-malnourished (blue dots) patients with gastric cancer. ESI (+): Positive ion mode, $R^2Y=0.698$, $Q^2=0.430$; ESI (-): Negative ion mode. $R^2Y=0.441$, $Q^2=0.328$. (**B**) Permutation tests: All blue Q^2 values on the left are lower than the original point on the right and the blue regression line at point Q^2 intersects the vertical axis (left side) at or below zero

glycerophospholipid metabolism; phenylalanine, tyrosine, and tryptophan biosynthesis; tyrosine metabolism; ubiquinone and other terpenoid-quinone biosynthesis; phenylalanine metabolism; and purine metabolism. See Fig. 5 and Table S1 for more details.

A predictive model of malnutrition in patients with gastric cancer

As displayed in Fig. 6, four metabolites, i.e., indoleacrylic acid, LysoPC(18:3/0:0), L-tryptophan, and LysoPC(20:3/0:0), clearly achieved greater significance (>7) than the other metabolites between malnourished and non- malnourished patients with gastric cancer. A predictive model of malnutrition in patients with gastric cancer was established based on these four metabolites to screen malnutrition. The corresponding ROC curve had an area under the curve (AUC) of 0.702 (95% CI: 0.651–0.768).

Discussion

This study explored serum fingerprinting of malnutrition in patients with gastric cancer based on non-targeted metabolomics using LC-MS analysis. We annotated 25 significantly differential metabolites that had lower intensities and two higher in malnourished patients with gastric cancer as compared with those non-malnourished. We matched eight metabolic pathways associated with malnutrition based on the 27 annotated significantly differential metabolites identified between malnourished and non-malnourished patients with gastric cancer. A reliable predictive model of malnutrition was developed based on the intensities of metabolites with the highest importance between malnourished and non-malnourished patients with gastric cancer.

Literature indicated that few metabolomics studies were performed on malnutrition in patients with cancer, whereas some metabolomics studies investigated

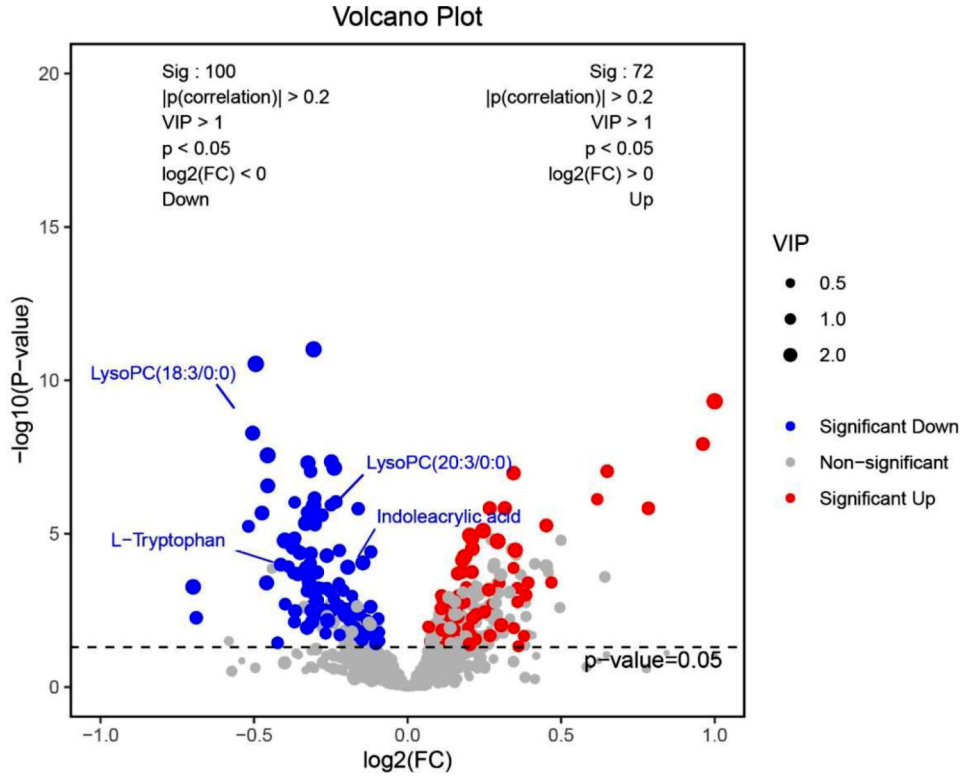

Fig. 2 Volcano plot of metabolites between malnourished and non-malnourished patients with gastric cancer. Red dots are significantly up-regulated differential metabolites (VIP > 1, |p(correlation)| >0.2, and $p < 0.05$) and blue dots are significantly down-regulated differential metabolites (VIP > 1, |p(correlation)| >0.2, and $p < 0.05$)

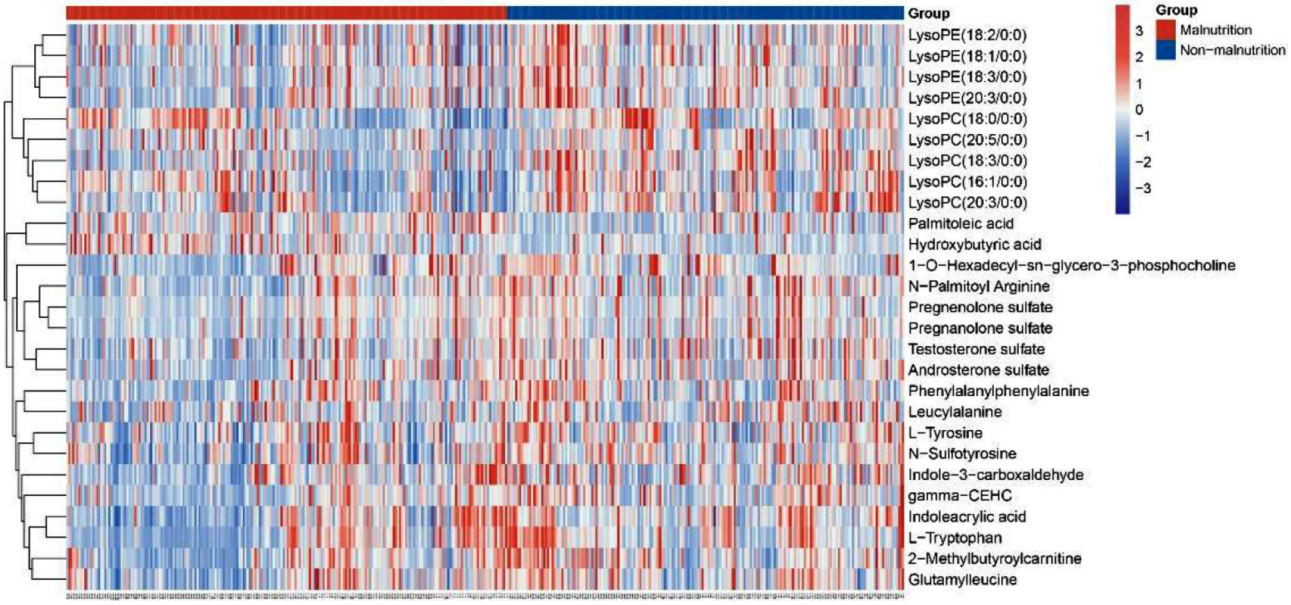

Fig. 3 Heatmap of serum levels of 27 annotated significantly differential metabolites (VIP > 1, |p(correlation)| >0.2, and $p < 0.05$) between malnourished and non-malnourished patients with gastric cancer. The colour from blue to red indicates that the peak intensity of the significantly differential metabolite is from low to high, i.e., the redder the significantly differential metabolite, the higher the peak intensity of the significantly differential metabolite. The peak intensities of metabolites were normalized by sum

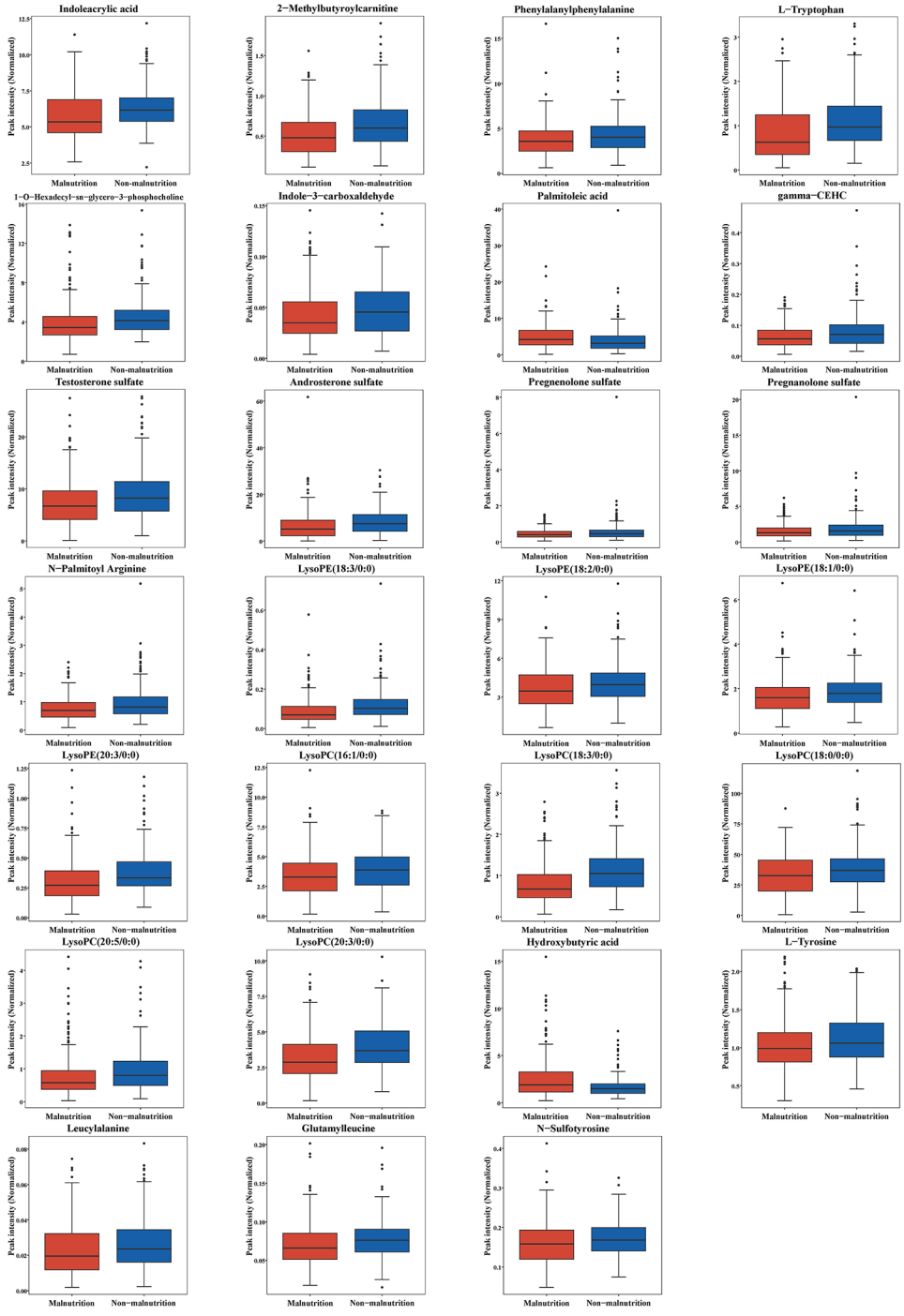

Fig. 4 Box-and-whisker plots of serum levels of 27 annotated significantly differential metabolites (VIP > 1, |p(correlation)| >0.2, and $p < 0.05$) between malnourished and non-malnourished patients with gastric cancer. The peak intensities of metabolites were normalized by sum

cachexia in patients with cancer [21]. Our research extended the current understanding of malnutrition. It revealed both novel and previously established significantly differential metabolites in patients with gastric cancer suffering from malnutrition compared to those without malnutrition. Newly identified significantly differential metabolites include indoleacrylic acid, 2-methylbutyroylcarnitine, phenylalanylphenylalanine, 1-O-hexadecyl-sn-glycero-3-phosphocholine, indole-3-carboxaldehyde, leucylalanine, glutamylleucine, N-sulfotyrosine, gamma-CEHC, testosterone sulfate, androsterone sulfate, pregnenolone sulfate, pregnanolone sulfate, N-palmitoyl arginine, LysoPE(18:3/0:0), LysoPC(18:3/0:0), LysoPC(20:5/0:0), hydroxybutyric acid

Table 2 The annotated significantly differential metabolites between malnourished and non-malnourished patients with gastric cancer

Metabolites	Formula	Variable importance in the projection (VIP)	*p* (correlation)	*p* value	Fold change (FC)	Retention time (RT)	Ion mode	Mass-to-change ratio (m/z)	Calculated m/z	Part per million (PPM)	Fragments
Indoleacrylic acid	C11H9NO2	2.48	0.26	0.0001	0.90	3.15	M+H	188.0701	188.0706	-2.7	143, 118, 91
2-Methylbutyroylcarnitine	C12H23NO4	1.95	0.21	0.0024	0.79	3.91	M+H	246.1675	246.1700	-10.1	85
Phenylalanylphenylalanine	C18H20N2O3	2.18	0.23	0.0036	0.87	4.73	M+H	313.1528	313.1547	-6.0	120, 103
L-Tryptophan	C11H12N2O2	2.29	0.24	0.0045	0.76	3.12	2 M+H	409.1866	409.1870	-1.1	143, 118
1-O-Hexadecyl-sn-glycero-3-phosphocholine	C24H52NO6P	2.77	0.29	0.0000	0.87	12.50	M+H	482.3604	482.3605	-0.2	482, 184, 104
Hydroxybutyric acid	C4H8O3	1.83	-0.31	0.0000	1.57	1.54	M-H	103.0387	103.0401	-13.3	57
Indole-3-carboxaldehyde	C9H7NO	1.22	0.21	0.0264	0.88	5.66	M-H	144.0452	144.0455	-2.0	144, 116, 115
L-Tyrosine	C9H11NO3	1.25	0.21	0.0195	0.93	1.71	M-H	180.0650	180.0666	-9.0	163, 119, 93
Leucylalanine	C9H18N2O3	1.29	0.22	0.0034	0.84	2.30	M-H	201.1237	201.1245	-3.8	139
Palmitoleic acid	C16H30O2	1.39	-0.24	0.0017	1.28	17.10	M-H	253.2152	253.2173	-8.3	253
Glutamylleucine	C11H20N2O5	1.55	0.26	0.0044	0.90	3.56	M-H	259.1297	259.1300	-1.0	130
N-Sulfotyrosine	C9H11NO6S	1.20	0.20	0.0314	0.94	1.84	M-H	260.0220	260.0234	-5.5	180, 119, 93, 79
gamma-CEHC	C15H20O4	1.55	0.26	0.0002	0.77	7.75	M-H	263.1289	263.1289	0.1	219, 151
Testosterone sulfate	C19H28O5S	2.17	0.37	0.0001	0.80	7.27	M-H	367.1568	367.1585	-4.5	367, 96
Androsterone sulfate	C19H30O5S	2.17	0.37	0.0075	0.81	7.79	M-H	369.1730	369.1741	-3.0	369, 96
Pregnenolone sulfate	C21H32O5S	1.56	0.27	0.0075	0.77	9.15	M-H	395.1881	395.1898	-4.2	395, 96
Pregnanolone sulfate	C21H34O5S	2.03	0.34	0.0033	0.78	8.13	M-H	397.2024	397.2054	-7.6	397, 96
N-Palmitoyl Arginine	C21H34O6S	2.46	0.42	0.0000	0.77	6.81	M-H	413.1982	413.2003	-5.2	413, 96
LysoPE(18:3/0:0)	C23H42NO7P	1.95	0.33	0.0001	0.75	10.64	M-H	474.2612	474.2626	-3.0	474, 277
LysoPE(18:2/0:0)	C23H44NO7P	1.50	0.26	0.0030	0.89	11.51	M-H	476.2736	476.2783	-9.8	476, 279
LysoPE(18:1/0:0)	C23H46NO7P	1.44	0.25	0.0147	0.90	13.31	M-H	478.2922	478.2939	-3.6	478, 281
LysoPE(20:3/0:0)	C25H46NO7P	2.11	0.36	0.0000	0.80	12.27	M-H	502.2887	502.2939	-10.4	502, 305, 196
LysoPC(16:1/0:0)	C24H48NO7P	1.53	0.26	0.0067	0.88	10.97	M+FA-H	538.3126	538.3150	-4.5	478, 253
LysoPC(18:3/0:0)	C26H48NO7P	2.48	0.42	0.0000	0.70	10.69	M+FA-H	562.3143	562.3150	-1.3	502, 277
LysoPC(18:0/0:0)	C26H54NO7P	1.26	0.21	0.0027	0.87	14.97	M+FA-H	568.3570	568.3620	-8.8	508, 283, 224
LysoPC(20:5/0:0)	C28H48NO7P	1.31	0.22	0.0178	0.83	10.07	M+FA-H	586.3132	586.3150	-3.1	526, 301, 224
LysoPC(20:3/0:0)	C28H52NO7P	1.88	0.32	0.0000	0.81	12.32	M+FA-H	590.3431	590.34634	-5.5	530, 305, 224

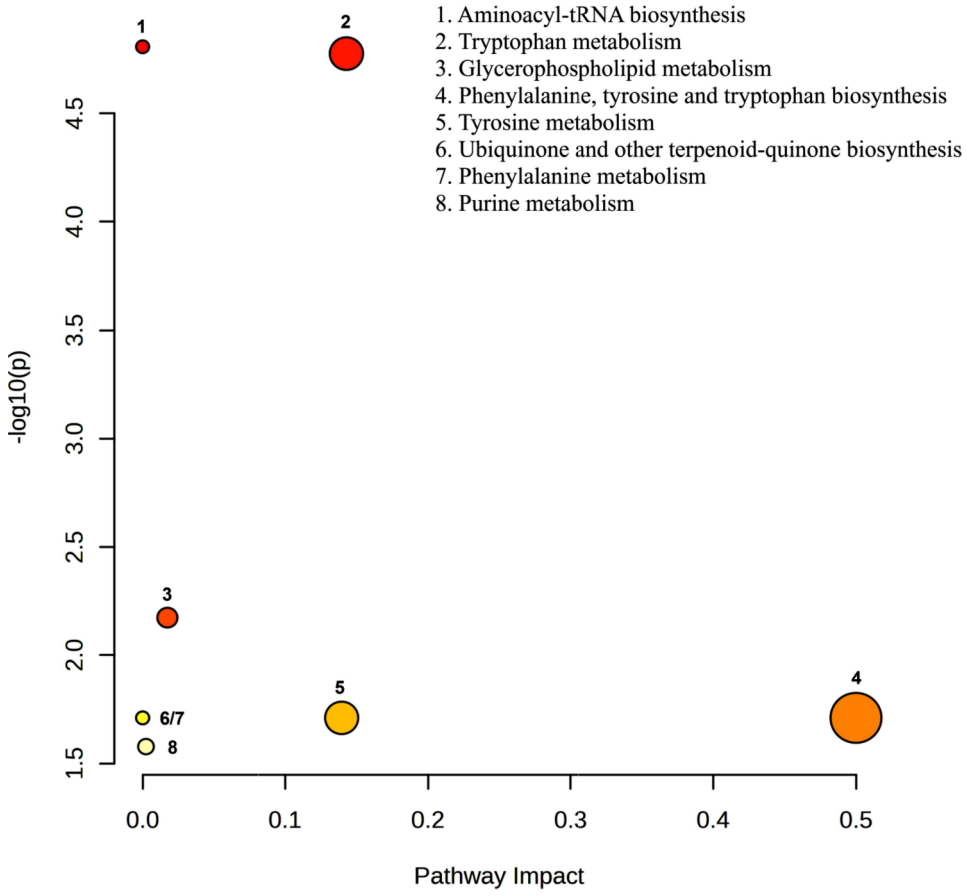

Fig. 5 Bubble diagram of the 8 metabolic pathways associated with malnutrition in patients with gastric cancer. The larger the bubble, the smaller the *p*-value; the redder the colour, the greater the significance

and palmitoleic acid. The intensities of most of these annotated significantly differential metabolites were lower in patients with malnutrition than those without malnutrition, including significantly differential metabolites indoleacrylic acid, LysoPC(18:3/0:0), L-tryptophan, and LysoPC(20:3/0:0), which were used to develop the prediction model of malnutrition in patients with gastric cancer.

Tryptophan, an aromatic amino acid, is essential for protein synthesis in humans and must be obtained exclusively through their diet [32]. In cases of malnutrition, the reduced availability of tryptophan can potentially heighten the risks for patients [33]. Decreased L-tryptophan in malnourished patients leads to impairment of the tryptophan-NAD+pathway, resulting in a decrease in NAD+, which may lead to liver dysfunction and further exacerbation of malnutrition [34]. In addition, L-tryptophan is thought to regulate skeletal muscle mass [35], and therefore a decrease in the biosynthetic pathway of tryptophan may contribute to sarcopenia [36]. Existing research indicates increased body mass index correlated positively with tryptophan levels, though the role of tryptophan and its metabolites in malnutrition remains poorly understood [33]. Numerous studies have explored the utilization of tryptophan from various sources by both humans and animals, with some of these reports emphasizing the potential for tryptophan supplementation or fortification [37]. A recent study reported treatment with 1-methyl-tryptophan, a compound that inhibits tryptophan degradation, in cachectic murine models successfully restored plasma tryptophan levels [38]. Cala et al. and Ni et al. also found that plasma tryptophan levels were lower in cachectic than in non-cachectic patients with cancer [23, 26].

Indoleacrylic acid, a metabolite of tryptophan, influences membrane unsaturated fatty acid levels by modulating cell lysophospholipase activity [39]. Due to this, notable alterations in the ratio of phosphatidylethanolamine to phospatidycholine, coupled with low indoleacrylic acid levels, may serve as indicators of cellular membrane permeability damage [40]. Increasing indoleacrylic acid production can stimulate an anti-inflammatory response, offering therapeutic benefits for inflammatory bowel disease [41]. Building upon this observation, we postulate that the decline in indoleacrylic acid levels results in dysfunction of the

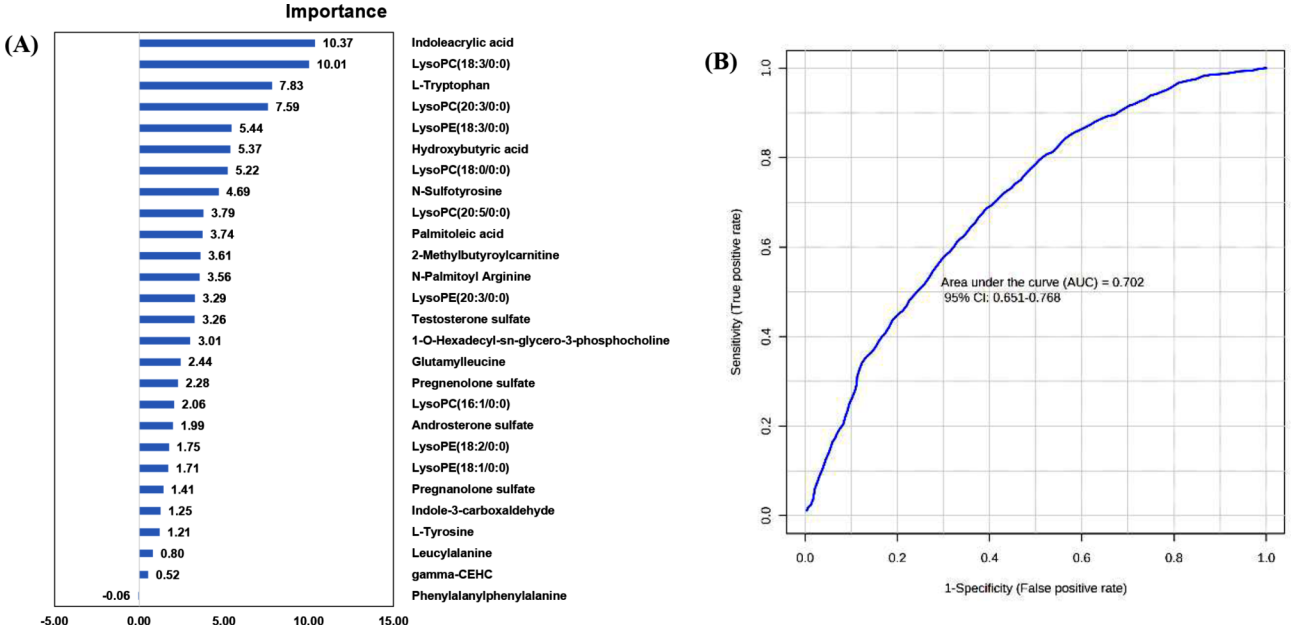

Fig. 6 Importance of significantly differential metabolites and predictive model for malnutrition in patients with gastric cancer. (**A**) importance of 27 annotated significantly differential metabolites (VIP > 1, |p(correlation)| >0.2, and $p < 0.05$) between malnourished and non-malnourished patients with gastric cancer based on random forest analysis. (**B**) ROC curves of the malnutrition predictive model in patients with gastric cancer based on indoleacrylic acid, LysoPC(18:3/0:0), L-tryptophan, and LysoPC(20:3/0:0)

intestinal epithelial barrier and provokes an inflammatory response, ultimately contributing to the onset of malnutrition. There isn't a substantial body of research specifically examining the effects of indoleacrylic acid on cancer cachexia and malnutrition, and further studies may be warranted to delve deeper into the topic.

LPC can stimulate the migration of lymphocytes and macrophages, elevate the production of pro-inflammatory cytokines, trigger oxidative stress, and facilitate apoptosis, thus exacerbating inflammation and fostering the development of diseases [42]. Low plasma levels of LPC specifically LPC(16:1) and LPC(20:3), in humans, are correlated with diminished mitochondrial oxidative capacity in skeletal muscle [43]. This dysregulation has also been implicated in the muscle atrophy observed in tumor-bearing animals [44]. Morigny et al., Ni et al., and Cala et al. reported that patients with cancer cachexia had lower plasma levels of numerous LPC species compared to patients without cancer cachexia, including LPC(20:3) [23, 25, 26]. Taylor et al.'s study also shown the concentration of plasma LPC is diminished in cancer patients experiencing weight loss and exhibiting activated inflammatory status [45].

We matched eight metabolic pathways associated with malnutrition in patients with gastric cancer. Two of the eight metabolic pathways, aminoacyl-tRNA biosynthesis and tryptophan metabolism, were matched based on L-tryptophan. Aminoacyl-tRNA biosynthesis was matched as a cachexia-related metabolic pathway in patients with cancer by More et al., Cala et al., and Yang et al. [23, 28, 46]. Glycerophospholipid metabolism was matched based on LPC(20:3), which was previously matched as a cachexia-related metabolic pathway in patients with cancer cachexia by Yang et al. [28]. All these findings further validate the robustness of the results of this study. Our study has contributed new findings because little research exists regarding the relationship between malnutrition and tryptophan metabolism.

A major contribution of this study is that we developed a predictive model associated with malnutrition based on the four annotated significantly differential metabolites with top importance, indoleacrylic acid, LysoPC(18:3/0:0), L-tryptophan, and LysoPC(20:3/0:0), between malnourished and non-malnourished patients with gastric cancer. Yang et al. also reported a distinct diagnostic model for cachexia screening in patients with cancer, and the corresponding ROC curve had an AUC of 0.991 using levels of carnosine, leucine, and phenyl acetate [28]. Miller et al. indicated a correlation between predicted and actual weight change with a combination profile of LysoPC(18:2), L-proline, hexadecanoic acid, octadecanoic acid, phenylalanine, and LysoPC(16:1) [47]. More et al. developed a predictive model of cachexia in patients with cancer based on 10 non-annotated and 5 annotated metabolites (erythronic acid, lactic acid, maltose, methionine, and ornithine) [46]. Various studies identified different differential metabolites to use when constructing predictive models, which may be related to the different study populations. Given the variability of metabolism in different tumor

types, our study included only patients with gastric cancer, which is one of the strengths of this study. Future relevant studies should focus on patients with the same tumor type, or even patients with the same tumor type at the same treatment stage, whenever possible.

This study has several limitations. First, all study subjects were from the same hospital. The results of this study may not be directly extrapolated to other patients with gastric cancer, considering geographic, ethnic, and other factors. Second, the subjects in this study were at different stages of treatment. Anti-cancer treatment may affect the metabolism of the patients. Third, we only tested for significantly differential metabolites in patient serum. These significantly differential metabolites were not validated in other biological specimens. Fourth, the results of this study were obtained from non-targeted analyses. Further research is needed to verify the top altered metabolites of malnourished compared to non-malnourished patients in a targeted analysis, providing specific concentrations. However, this is a large sample untargeted metabolomics study in patients with gastric cancer. The significance of our sample size can be appraised by comparison with the previous similar studies.

Conclusion

In conclusion, 25 of the 27 annotated significantly differential metabolite intensities were low in malnourished compared to non-malnourished patients with gastric cancer, indicating lower differences in metabolite intensities from non-malnutrition to malnutrition with several new significantly differential metabolites. Based on the annotated significantly differential metabolites identified between gastric cancer patients with and without malnutrition, eight metabolic pathways associated with malnutrition were matched, informing molecular mechanisms of malnutrition in patients with gastric cancer. We developed a predictive model of malnutrition in patients with gastric cancer based on the intensities of four annotated significantly differential metabolites, providing empirical evidence for malnutrition assessment, especially for patients who are unable to provide necessary information on the clinical prediction or diagnosis of malnutrition. These findings may inform biomarkers for malnutrition prediction or diagnosis and medications or interventions for malnutrition prevention or treatment in patients with gastric cancer.

Abbreviations

AUC	Area under the curve
BMI	Body mass index
BPC	Base peak chromatograms
CC	Calf circumference
CI	Confidence interval
ECOG-PS	Eastern Cooperative Oncology Group Performance Status
GLIM	Global Leadership Initiative on Malnutrition
LC-MS	Liquid chromatography-mass spectrometry
LysoPC	Lysophosphatidylcholine
NRS 2002	Nutritional Risk Screening 2002
OPLS-DA	Orthogonal partial least-squares discriminant analysis
PCA	Principal component analysis
PPM	Part per million
QC	Quality control
ROC	Receiver operating characteristic
RSD	Relative standard deviation
RT	Retention time
VIP	Variable importance in the projection

Supplementary Information

The online version contains supplementary material available at https://doi.org/10.1186/s12885-024-12964-6.

Supplementary Material 1

Supplementary Material 2

Acknowledgements

The authors would like to thank all the patients, staff, and students who participated in this study. The authors are particularly grateful to Ms. Kim Marie Renfro at the University of Texas Health Science Center at San Antonio for her editorial support.

Author contributions

L.F.: Conceptualization, investigation, data curation, formal analysis, funding acquisition, methodology, software, project administration, and writing original draft. L.S. and C.C.: Conceptualization, resources, and writing review and editing. X.Z. and L.C.: Data curation, formal analysis, methodology, software, and writing original draft. L.Z., D.H., Y.H., and D.G.: Investigation, data curation, project administration, and resources. S.Z.: Investigation, data curation, funding acquisition, project administration, and resources. X.Y. and S.Y.: Conceptualization, supervision, validation, visualization, resources, and writing review and editing. All authors contributed to and approved the final version of the manuscript.

Funding

The Explore Public Welfare Project of Zhejiang Province Natural Science Foundation (LTGY23H160026), the General Project of Zhejiang Province Medical Science and Technology Plan (2022KY1331), and the Major Project of Jinhua City Science and Technology Research Plan (2021-3-051), China supported this study.

Data availability

The datasets used during the current study are available from the corresponding authors on reasonable request.

Declarations

Ethics approval and consent to participate

We obtained ethics approvals from the Medical Ethics Committee of Jinhua Municipal Central Hospital (Affiliated Jinhua Hospital, Zhejiang University School of Medicine) ((Research)2022-Ethical Review-210, (Research)2021-Ethical Review – 142, and (Research)2020-Ethical Review – 298). All participants provided written informed consent before any research activities commenced.

Consent for publication

Not applicable.

Competing interests

The authors declare that they have no competing interests.

Author details

[1]Department of Nursing, Affiliated Jinhua Hospital, Zhejiang University School of Medicine, Jinhua 321000, China
[2]Central Laboratory, Affiliated Jinhua Hospital, Zhejiang University School of Medicine, Jinhua 321000, China

[3]School of Nursing, The University of Texas Health Science Center at San Antonio (UTHSCSA), San Antonio 78229, USA
[4]Institute of Analysis, Guangdong Academy of Sciences (China National Analytical Center), Guangzhou, Guangzhou 510070, China
[5]Department of Pathology, Affiliated Jinhua Hospital, Zhejiang University School of Medicine, Jinhua 321000, China
[6]Department of Gastrointestinal Surgery, Affiliated Jinhua Hospital, Zhejiang University School of Medicine, Jinhua 321000, China
[7]Department of Hepatobiliary and Pancreatic Surgery, Affiliated Jinhua Hospital, Zhejiang University School of Medicine, Jinhua 321000, China

Received: 19 April 2024 / Accepted: 18 September 2024
Published online: 27 September 2024

References

1. Sung H, Ferlay J, Siegel RL, Laversanne M, Soerjomataram I, Jemal A, Bray F. Global Cancer statistics 2020: GLOBOCAN estimates of incidence and Mortality Worldwide for 36 cancers in 185 countries. CA Cancer J Clin. 2021;71:209–49.
2. Cao W, Chen HD, Yu YW, Li N, Chen WQ. Changing profiles of cancer burden worldwide and in China: a secondary analysis of the global cancer statistics 2020. Chin Med J (Engl). 2021;134:783–91.
3. Xia C, Dong X, Li H, Cao M, Sun D, He S, Yang F, Yan X, Zhang S, Li N, Chen W. Cancer statistics in China and United States, 2022: profiles, trends, and determinants. Chin Med J (Engl). 2022;135:584–90.
4. Tuo JY, Bi JH, Yuan HY, Jiang YF, Ji XW, Li HL, Xiang YB. Trends of stomach cancer survival: a systematic review of survival rates from population-based cancer registration. J Dig Dis. 2022;23:22–32.
5. Li H, Zhang H, Zhang H, Wang Y, Wang X, Hou H. Global Health Epidemiology Reference G: survival of gastric cancer in China from 2000 to 2022: a nationwide systematic review of hospital-based studies. J Glob Health. 2022;12:11014.
6. Hebuterne X, Lemarie E, Michallet M, de Montreuil CB, Schneider SM, Goldwasser F. Prevalence of malnutrition and current use of nutrition support in patients with cancer. JPEN J Parenter Enter Nutr. 2014;38:196–204.
7. Marshall KM, Loeliger J, Nolte L, Kelaart A, Kiss NK. Prevalence of malnutrition and impact on clinical outcomes in cancer services: a comparison of two time points. Clin Nutr. 2019;38:644–51.
8. Landgrebe M, Tobberup R, Carus A, Rasmussen HH. GLIM diagnosed malnutrition predicts clinical outcomes and quality of life in patients with non-small cell lung cancer. Clin Nutr. 2023;42:190–8.
9. Maia FCP, Silva TA, Generoso SV, Correia M. Malnutrition is associated with poor health-related quality of life in surgical patients with gastrointestinal cancer. Nutr. 2020;75–76:110769.
10. Zheng HL, Lu J, Li P, Xie JW, Wang JB, Lin JX, Chen QY, Cao LL, Lin M, Tu R, et al. Effects of Preoperative Malnutrition on short- and long-term outcomes of patients with gastric Cancer: can we do better? Ann Surg Oncol. 2017;24:3376–85.
11. Maasberg S, Knappe-Drzikova B, Vonderbeck D, Jann H, Weylandt KH, Grieser C, Pascher A, Schefold JC, Pavel M, Wiedenmann B, et al. Malnutrition predicts clinical outcome in patients with neuroendocrine neoplasia. Neuroendocrinology. 2017;104:11–25.
12. Freijer K, Tan SS, Koopmanschap MA, Meijers JM, Halfens RJ, Nuijten MJ. The economic costs of disease related malnutrition. Clin Nutr. 2013;32:136–41.
13. Luboš S. Basics in Clinical Nutrition. Fifth ed. Prague: Galen; 2019.
14. Cederholm T, Jensen GL, Correia M, Gonzalez MC, Fukushima R, Higashiguchi T, Baptista G, Barazzoni R, Blaauw R, Coats A, et al. GLIM criteria for the diagnosis of malnutrition - A consensus report from the global clinical nutrition community. Clin Nutr. 2019;38:1–9.
15. Zhang Z, Wan Z, Zhu Y, Zhang L, Zhang L, Wan H. Prevalence of malnutrition comparing NRS2002, MUST, and PG-SGA with the GLIM criteria in adults with cancer: a multi-center study. Nutrition. 2021;83:111072.
16. Arends J, Baracos V, Bertz H, Bozzetti F, Calder PC, Deutz NEP, Erickson N, Laviano A, Lisanti MP, Lobo DN, et al. ESPEN expert group recommendations for action against cancer-related malnutrition. Clin Nutr. 2017;36:1187–96.
17. Klassen A, Faccio AT, Canuto GA, da Cruz PL, Ribeiro HC, Tavares MF, Sussulini A. Metabolomics: definitions and significance in Systems Biology. Adv Exp Med Biol. 2017;965:3–17.
18. Ivanisevic J, Thomas A. Metabolomics as a Tool to understand pathophysiological processes. Methods Mol Biol. 2018;1730:3–28.
19. Humphry NA, Wilson T, Cox MC, Carter B, Arkesteijn M, Reeves NL, Brakenridge S, McCarthy K, Bunni J, Draper J, Hewitt J. Association of Postoperative Clinical outcomes with Sarcopenia, Frailty, and Nutritional Status in older patients with Colorectal Cancer: protocol for a prospective cohort study. JMIR Res Protoc. 2021;10:e16846.
20. Cederholm T, Barazzoni R, Austin P, Ballmer P, Biolo G, Bischoff SC, Compher C, Correia I, Higashiguchi T, Holst M, et al. ESPEN guidelines on definitions and terminology of clinical nutrition. Clin Nutr. 2017;36:49–64.
21. Fu L, Chen L, Li R, Xu W, Fu J, Ye X. Metabolomics studies on cachexia in patients with cancer: a scoping review protocol. BMJ Open. 2022;12:e052125.
22. Fearon K, Strasser F, Anker SD, Bosaeus I, Bruera E, Fainsinger RL, Jatoi A, Loprinzi C, MacDonald N, Mantovani G, et al. Definition and classification of cancer cachexia: an international consensus. Lancet Oncol. 2011;12:489–95.
23. Cala MP, Agullo-Ortuno MT, Prieto-Garcia E, Gonzalez-Riano C, Parrilla-Rubio L, Barbas C, Diaz-Garcia CV, Garcia A, Pernaut C, Adeva J, et al. Multiplatform plasma fingerprinting in cancer cachexia: a pilot observational and translational study. J Cachexia Sarcopenia Muscle. 2018;9:348–57.
24. Catanese S, Beuchel CF, Sawall T, Lordick F, Brauer R, Scholz M, Ceglarek U, Hacker UT. Biomarkers related to fatty acid oxidative capacity are predictive for continued weight loss in cachectic cancer patients. J Cachexia Sarcopenia Muscle. 2021;12:2101–10.
25. Morigny P, Zuber J, Haid M, Kaltenecker D, Riols F, Joanna DCL, Simoes E, Otoch JP, Schmidt SF, Herzig S, et al. High levels of modified ceramides are a defining feature of murine and human cancer cachexia. J Cachexia Sarcopenia Muscle. 2020;11:1459–75.
26. Ni Y, Lohinai Z, Heshiki Y, Dome B, Moldvay J, Dulka E, Galffy G, Berta J, Weiss GJ, Sommer MOA, Panagiotou G. Distinct composition and metabolic functions of human gut microbiota are associated with cachexia in lung cancer patients. ISME J. 2021;15:3207–20.
27. Boguszewicz L, Bielen A, Mrochem-Kwarciak J, Skorupa A, Ciszek M, Heyda A, Wygoda A, Kotylak A, Skladowski K, Sokol M. NMR-based metabolomics in real-time monitoring of treatment induced toxicity and cachexia in head and neck cancer: a method for early detection of high risk patients. Metabolomics. 2019;15:110.
28. Yang QJ, Zhao JR, Hao J, Li B, Huo Y, Han YL, Wan LL, Li J, Huang J, Lu J, et al. Serum and urine metabolomics study reveals a distinct diagnostic model for cancer cachexia. J Cachexia Sarcopenia Muscle. 2018;9:71–85.
29. Ose J, Gigic B, Lin T, Liesenfeld DB, Böhm J, Nattenmüller J, Scherer D, Lin Z, Schrotz-King P, Habermann N, et al. Multiplatform urinary metabolomics profiling to Discriminate Cachectic from Non-cachectic Colorectal Cancer patients: Pilot results from the ColoCare Study. Metabolites. 2019;9:178.
30. Meza-Valderrama D, Marco E, Davalos-Yerovi V, Muns MD, Tejero-Sanchez M, Duarte E, et al. Sarcopenia, malnutrition, and cachexia: adapting definitions and terminology of Nutritional disorders in older people with Cancer. Nutr. 2021;13:761.
31. Fu L, Xu X, Zhang Y, Jin J, Zhu S, Shi H, Guan Q, Zhang L, Hu Y, Zhuang B, et al. Agreements between GLIM using left calf circumference as criterion for reduced muscle mass and PG-SGA, and GLIM using ASMI for the diagnosis of malnutrition in gastric cancer patients. Nutr Hosp. 2024;4:1–34.
32. Lavelle A, Sokol H. Gut microbiota-derived metabolites as key actors in inflammatory bowel disease. Nat Rev Gastroenterol Hepatol. 2020;17:223–37.
33. Ritz J, Wunderle C, Stumpf F, Laager R, Tribolet P, Neyer P, Bernasconi L, Stanga Z, Mueller B, Schuetz P. Association of tryptophan pathway metabolites with mortality and effectiveness of nutritional support among patients at nutritional risk: secondary analysis of a randomized clinical trial. Front Nutr. 2024;11:1335242.
34. Hu G, Ling C, Chi L, Thind MK, Furse S, Koulman A, Swann JR, Lee D, Calon MM, Bourdon C, et al. The role of the tryptophan-NAD + pathway in a mouse model of severe malnutrition induced liver dysfunction. Nat Commun. 2022;13:7576.
35. Ninomiya S, Nakamura N, Nakamura H, Mizutani T, Kaneda Y, Yamaguchi K, et al. Low levels of serum tryptophan underlie skeletal muscle atrophy. Nutr. 2020;12:978.
36. Wang Y, Zhang Y, Lane NE, Wu J, Yang T, Li J, He H, Wei J, Zeng C, Lei G. Population-based metagenomics analysis reveals altered gut microbiome in Sarcopenia: data from the Xiangya Sarcopenia Study. J Cachexia Sarcopenia Muscle. 2022;13:2340–51.
37. Friedman M. Analysis, Nutrition, and Health benefits of Tryptophan. Int J Tryptophan Res. 2018;11:1178646918802282.
38. Agullo-Ortuno MT, Mancebo E, Grau M, Nunez Sobrino JA, Paz-Ares L, Lopez-Martin JA, et al. Tryptophan modulation in Cancer-Associated Cachexia Mouse models. Int J Mol Sci. 2023;24:13005.

39. Bell JG, Sargent JR, Tocher DR, Dick JR. Red blood cell fatty acid compositions in a patient with autistic spectrum disorder: a characteristic abnormality in neurodevelopmental disorders? Prostaglandins Leukot Essent Fat Acids. 2000;63:21–5.
40. Andrade F, Sánchez-Ortega A, Llarena M, Pinar-Sueiro S, Galdós M, Goicolea MA, Barrio RJ, Aldámiz-Echevarría L. Metabolomics in non-arteritic anterior ischemic optic neuropathy patients by liquid chromatography–quadrupole time-of-flight mass spectrometry. Metabolomics. 2014;11:468–76.
41. Wlodarska M, Luo C, Kolde R, d'Hennezel E, Annand JW, Heim CE, Krastel P, Schmitt EK, Omar AS, Creasey EA, et al. Indoleacrylic Acid produced by Commensal Peptostreptococcus Species suppresses inflammation. Cell Host Microbe. 2017;22:25–e3726.
42. Liu P, Zhu W, Chen C, Yan B, Zhu L, Chen X, Peng C. The mechanisms of lysophosphatidylcholine in the development of diseases. Life Sci. 2020;247:117443.
43. Semba RD, Zhang P, Adelnia F, Sun K, Gonzalez-Freire M, Salem N Jr., Brennan N, Spencer RG, Fishbein K, Khadeer M, et al. Low plasma lysophosphatidylcholines are associated with impaired mitochondrial oxidative capacity in adults in the Baltimore Longitudinal Study of Aging. Aging Cell. 2019;18:e12915.
44. Carson JA, Hardee JP, VanderVeen BN. The emerging role of skeletal muscle oxidative metabolism as a biological target and cellular regulator of cancer-induced muscle wasting. Semin Cell Dev Biol. 2016;54:53–67.
45. Taylor LA, Arends J, Hodina AK, Unger C, Massing U. Plasma lyso-phosphatidylcholine concentration is decreased in cancer patients with weight loss and activated inflammatory status. Lipids Health Dis. 2007;6:17.
46. More TH, Hiller K, Seifert M, Illig T, Schmidt R, Gronauer R, von Hahn T, Weilert H, Stang A. Metabolomics analysis reveals novel serum metabolite alterations in cancer cachexia. Front Oncol. 2024;14:1286896.
47. Miller J, Alshehri A, Ramage MI, Stephens NA, Mullen AB, Boyd M, Ross JA, Wigmore SJ, Watson DG, Skipworth RJE. Plasma Metabolomics identifies lipid and amino acid markers of weight loss in patients with Upper Gastrointestinal Cancer. Cancers. 2019;11:1594.

Publisher's note